Max-Planck-Institut
für Mathematik
in den Naturwissenschaften
Leipzig

Synchronizing chaotic neuromodules

by

Frank Pasemann

Preprint-Nr.: 13 1999

Synchronizing Chaotic Neuromodules *

Frank Pasemann
Max-Planck-Institute for Mathematics in the Sciences
D-04103 Leipzig, Germany
email: f.pasemann@mis.mpg.de

Abstract

We discuss the time-discrete parametrized synchronous dynamics of two coupled chaotic neuromodules. The symmetrical coupling of identical 2-neuron modules results in periodic, quasiperiodic as well as chaotic dynamics constrained to a synchronization manifold M. Stability of the synchonized dynamics is calculated by transversal Lyapunov exponents. In addition to synchronized attractors there often co-exist asynchronous periodic, quasiperiodic or even chaotic atractors. Simulation results for selected sets of parameters are presented.

*in: Proceedings of the ESANN'99, Bruges, April 21-23, to appear.

1 Introduction

Many recent articles investigated the feasibility of synchronized chaotic dynamics in various kinds of coupled systems (cf. citations in [1]). Most of this work was stimulated mainly because of its importance for applications in the field of secure communication. On the other hand, selective synchronization of neural activity in biological brains was often suggested to be a fundamental temporal mechanism for binding spatially distributed features into a coherent object (cf. e.g. [4]). Thus, studying the properties of synchronized dynamics in coupled chaotic neuromodules may provide interesting models also for the description of higher level information processing in biological and artificial neural systems. Coupled neuromodules provide a large set of parameters (synaptic weights and bias terms/stationary inputs), which allow not only synchronization but also the de-synchronization of module dynamics.

In the following we will use the term "synchronization" in the sense of *complete synchronization* of dynamical systems; i.e. we consider systems, the states of which can coincide, while the dynamics in time remains, for instance, chaotic. We also discern between global and local synchronization. Global synchronization means that for almost all initial conditions the orbits of the systems will synchronize. Local synchronization refers to stable synchronized states; i.e. small perturbations will not de-synchronize the systems.

In this contribution we study the discrete synchronous dynamics of two coupled neuromodules. The modules are composed of standard analog neurons: a self-inhibiting neuron coupled bi-directionally to an excitatory neuron. This setup has larger parameter domains allowing for chaotic module dynamics [2]. We derive conditions for the existence of synchronized dynamics in the coupled modules and for the stability of synchronized states. Already in this simple coupled system we observe global as well as local synchronization of periodic, quasiperiodic and chaotic dynamics. Synchronized orbits are not always stable; this be read from the *transversal* Lyapunov exponents introduced in section 2. The boundary between stable and unstable synchronization of chaos corresponds to switching from a chaotic to a hyperchaotic [3] regime of the coupled system. Furthermore, computer simulations demonstrate that various non-synchronous attractors may co-exist with attractors constrained to the synchronization manifold M.

2 Coupling chaotic neuromodules

We are considering a neuromodule as a discrete parametrized dynamical system on an n-dimensional activity phase space $\mathbf{R}^n$ given by the map

$$a_i(t+1) = \theta_i + \sum_{j=1}^{n} w_{ij}\, \sigma(a_j(t)) \;, \quad i = 1, \ldots, n \;, \tag{1}$$

where $a_i \in \mathbf{R}^n$ denotes the activity of the i-th neuron, and $\theta_i = \overline{\theta}_i + I_i$ denotes the sum of its fixed bias term $\overline{\theta}_i$ and its stationary external input I_i. The output $o_i = \sigma(a_i)$ of a unit is given by the standard sigmoidal transfer function $\sigma(x) := (1 + e^{-x})^{-1}$, $x \in \mathbf{R}$, and w_{ij} denotes the synaptic weight from unit j to unit i. A neuromodule having a parameter set $\rho = (\theta, w)$ for which the dynamics (1) has at least one chaotic attractor will be called a *chaotic neuromodule*.

In the following we consider a chaotic neuromodule consisting of an excitatory unit bi-directionally coupled to an inhibitory unit with self-connection [2]. Its 2-dimensional discrete dynamics is given by a five parameter family of maps $f_\rho : \mathbf{R}^2 \to \mathbf{R}^2$, $\rho = (\theta_1, w_{12}, \theta_2, w_{21}, w_{22}) \in \mathbf{R}^5$, defined by

$$\begin{aligned} a_1(t+1) &:= \theta_1 + w_{12}\,\sigma(a_2(t)) \quad , \\ a_2(t+1) &:= \theta_2 + w_{21}\,\sigma(a_1(t)) + w_{22}\,\sigma(a_2(t)) \quad . \end{aligned} \tag{2}$$

This module has a large parameter domain, where its dynamics has a global chaotic attractor, but also the coexistence of periodic and chaotic attractors is observed [2].

Now, let A and B denote two neuromodules of the kind described above (2) with parameter sets $\rho^A = (\theta^A, w^A)$ and $\rho^B = (\theta^B, w^B)$. The neural activities of module A and B will be denoted a_i, b_i, $i = 1, 2$, respectively. Connections going from module B to module A are given by (2×2)-coupling matrix w^{AB}. Correspondingly, connections from module A to module B are given as a matrix w^{BA}. We will discuss the special case of inhibitory couplings from the inhibitory neuron of a module to the excitatory neuron of the other module. The resulting 4-dimensional dynamics F_ρ of the coupled 2-modules A and B is then given by

$$\begin{aligned} a_1(t+1) &= \theta_1^A + w_{12}^A\,\sigma(a_2(t)) + w_{12}^{AB}\,\sigma(b_2(t)) \quad , \\ a_2(t+1) &= \theta_2^A + w_{21}^A\,\sigma(a_1(t)) + w_{22}^A\,\sigma(a_2(t)) \quad , \\ b_1(t+1) &= \theta_1^B + w_{12}^B\,\sigma(b_2(t)) + w_{12}^{BA}\,\sigma(a_2(t)) \quad , \\ b_2(t+1) &= \theta_2^B + w_{21}^B\,\sigma(b_1(t)) + w_{22}^B\,\sigma(b_2(t)) \quad . \end{aligned} \tag{3}$$

We are interested in the process of *complete synchronization* of module neurons, by which we mean that there exists a subset $D \subset \mathbf{R}^4$ such that $(a_0, b_0) \in D$ implies

$$\lim_{t\to\infty} \mid a(t; a_0) - b(t; b_0) \mid = 0 \ ,$$

where $(a(t; a_0), b(t; b_0))$ denotes the orbit under F_ρ through the initial condition $(a_0, b_0) \in \mathbf{R}^4$. Thus we will study the case where corresponding neurons of the modules have identical activities during a process. The synchronization is called *global* if $D \equiv \mathbf{R}^{2n}$, and *local* if $D \subset \mathbf{R}^4$ is a proper subset. Thus, a *synchronized state* s of the coupled system is defined by $s := a = b \in \mathbf{R}^n$. The *synchronization manifold* $M := \{(s, s) \in \mathbf{R}^{2n} \mid s = a = b\}$ of synchronized states corresponds to a 2-dimensional hyperplane $M \cong \mathbf{R}^2 \subset \mathbf{R}^4$. We introduce coordinates parallel

and orthogonal to the synchronization manifold M as follows:

$$\xi_i := \frac{1}{\sqrt{2}}(a_i + b_i) \quad , \quad \eta_i := \frac{1}{\sqrt{2}}(a_i - b_i) \quad , \quad i = 1, 2 \; . \tag{4}$$

For simplicity, we will now consider identical modules with parameter sets satisfying

$$\theta := \theta^A = \theta^B \; , \quad w := w^A = w^B \; , \quad w^{coup} := w^{BA} = w^{AB} \; . \tag{5}$$

Setting $\eta(t_0) = a(t_0) - b(t_0)) = 0$ for some t_0 we can immediately verify by direct calculation that every orbit of F_ρ through a synchronized state $s \in M$ is constrained to M for all times.

Using (ξ, η)-coordinates given by (4) the dynamics $\tilde{F}_\rho$ of two coupled identical modules can be written as

$$\xi_i(t+1) \;=\; \sqrt{2} \cdot \theta_i + \frac{1}{\sqrt{2}} \sum_{j=1}^{2} w_{ij}^{+} \cdot G^{+}(\xi_j(t), \eta_j(t)) \; , \quad i = 1, 2 \; , \tag{6}$$

$$\eta_i(t+1) \;=\; \frac{1}{\sqrt{2}} \sum_{j=1}^{2} w_{ij}^{-} \cdot G^{-}(\xi_j(t), \eta_j(t)) \; , \quad i = 1, 2 \; . \tag{7}$$

where we have set

$$w^{+} := (w + w^{coup}) \quad , \quad w^{-} := (w - w^{coup}) \; , \tag{8}$$

and the functions G^{+}, $G^{-} : \mathbf{R}^2 \to \mathbf{R}$ are defined by

$$G^{+}(x, y) := \sigma(\frac{1}{\sqrt{2}}(x + y)) + \sigma(\frac{1}{\sqrt{2}}(x - y)) \; , \tag{9}$$

$$G^{-}(x, y) := \sigma(\frac{1}{\sqrt{2}}(x + y)) - \sigma(\frac{1}{\sqrt{2}}(x - y)) \; . \tag{10}$$

Setting $\eta = 0$ and $s = 1/\sqrt{2}\,\xi$, the synchronized 2-dimensional dynamics F_ρ^s constrained to M is derived from equations (6). It reads

$$s_1(t+1) \;=\; \theta_1 + w_{12}^{+} \cdot \sigma(s_2(t)) \; , \tag{11}$$

$$s_2(t+1) \;=\; \theta_2 + w_{21}^{+} \cdot \sigma(s_1(t)) + w_{22}^{+} \cdot \sigma(s_2(t)) \; . \tag{12}$$

Thus, the synchronized dynamics F_ρ^s will display the whole spectrum of dynamical behavior of a single isolated chaotic 2-module with w_{12} in (2) replaced by $w_{12}^{+} = w_{12}^{A} + w_{12}^{AB}$; i.e. it may have fixed point attractors as well as periodic or chaotic ones [2]. Although the persistence of synchronized dynamics for identical modules is guaranteed by condition (5), it is not at all clear that the synchronization manifold M itself is asymptotically stable with respect to the dynamics $\tilde{F}_\rho$. Thus, a periodic or chaotic orbit in M may be an attractor for the synchronized dynamics F_ρ^s but not for the dynamics $\tilde{F}_\rho$ of the coupled system.

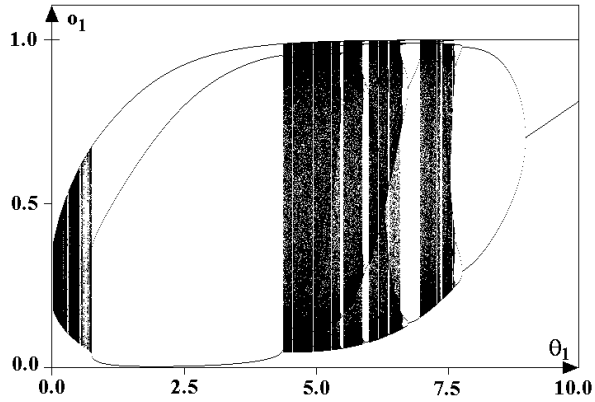

Figure 1: Bifurcation diagram for the synchronous dynamics with respect to θ_1 (= inputs to the excitatory units). For fixed parameter values see text.

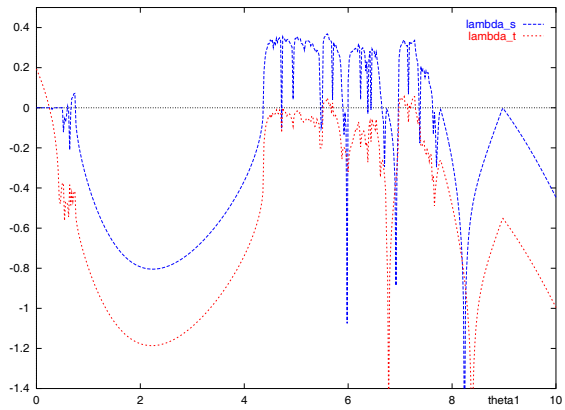

Figure 2: Largest synchronization and transversal exponents corresponding to the bifurcation diagram of figure 1.

To discuss the stability aspects of the synchronization manifold M it is effective to consider the *synchronization exponents* λ_i^s and the *transversal exponents* $\lambda_i^\perp$, $i = 1, 2$ for the synchronized dynamics (11). They are derived from the linearization $D\tilde{F}_\rho(s)$ of $\tilde{F}_\rho$ around synchronized states $s(t)$:

$$D\tilde{F}_\rho(s) = \begin{pmatrix} L^+(s) & 0 \\ 0 & L^-(s) \end{pmatrix}, \quad L_{ij}^\pm(s) := w_{ij}^\pm \cdot \sigma'(s_j), \quad i, j = 1, 2\,. \tag{13}$$

Synchronization exponents λ_i^s will be calculated from the eigenvalues of matrix L^+, and transversal exponents $\lambda_i^\perp$ from those of L^-. Synchronized chaotic dynamics will be characterized by a situation where at least one synchronization exponent satisfies $\lambda^s > 0$. On the other hand, a positive transversal exponent indicates an unstable synchronization manifold M. Thus, if an unstable M contains a chaotic orbit the system entered a *hyperchaotic* regime [3]; i.e. at least two Lyapunov exponents of the synchronized dynamics F_ρ^s are positive.

Simulations reveal that stable synchronization of identical 2-modules occurs over a large range of identical external inputs to the excitatory units; moreover, synchronization can be observed for periodic orbits as well as for quasi-periodic or chaotic dynamics. This is illustrated, for instance, in the bifurcation diagram of the synchronized dynamics constrained to M depicted for the fixed parameters $\theta_2 = -2$, $-w_{12} = w_{21} = 6$, $w_{22} = -16$, $w^{coup} = -3$ in figure (1). Control parameter is the external input θ_1 to the excitatory units. Starting at $\theta_1 = 0$, quasiperiodic orbits are observed, succeeded by a short interval with periodic and chaotic attractors. Then a large domain of period-3 attractors is seen, which at $\theta_1 = 4.38$ bifurcates into a chaotic attractor. A "classical" chaotic domain follows, where reversed period-doubling routes to chaos finally end up in period-2 attractors. The stability of this synchronous dynamics can be read from figure (2) where the largest synchronization and transversal exponents, λ_1^s and $\lambda_1^\perp$, respectively, are depicted. We observe θ_1-intervals for which the transversal exponent $\lambda_1^\perp$ is positive; i.e. the corresponding synchronized dynamics on M is unstable. The underlying data file locates the larger instability θ_1-intervals as $(0.0, 0.24)$, $(5.52, 5.66)$, $(6.98, 7.28)$.

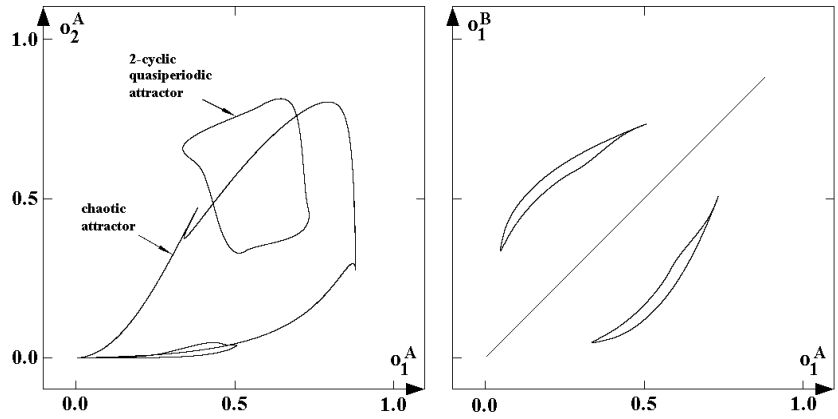

Figure 3: A synchronous chaotic attractor co-existing with an asynchronous quasiperiodic attractor for the coupled 2-neuron modules. Figures show projections to the phase space of module A (left) and to the (o_1^A, o_1^B)-output space of the coupled system. Parameters: see text.

We conclude that stability of synchronous periodic and chaotic dynamics in symmetrically coupled identical neuromodules is a quite general phenomenon. However, the following observation is also noteworthy: For large parameter domains there co-exist different attractors in the coupled system: There are synchronous periodic or chaotic attractors constrained to M and at the same time also asynchronous periodic, quasiperiodic or chaotic attractors not constrained to M. An example is shown in figure 3, where a synchronous chaotic attractor co-exists with an asynchronous quasiperiodic attractor for parameter values

$\theta_1 = 2$, $\theta_2 = -1$, $-w_{12} = w_{21} = 6$, $w_{22} = -16$, $w_{12}^{coup} = -3$. The left figure shows projections of the co-existing attractors onto the (o_1^A, o_2^A)-phase space of module A, the right hand figure projections onto the (o_1^A, o_1^B)-output space of the coupled system. Synchronized outputs will appear as states on the main diagonal in (o_1^A, o_1^B)-space.

3 Conclusions

Synchronized chaos in symmetrically coupled identical neuromodules is a fairly general phenomenon. It often co-exists with different kinds of asynchronous dynamics. Thus, stable synchronization can depend on initial conditions, that is, on the "history" of the coupled system. Furthermore, a synchronized mode often persists even if external inputs are varying slowly. Thus, synchronization of coupled modules is really a sign for time-varying (identical) input signals with amplitudes having a *fixed ratio* (recall, that the inputs may correspond to the weighted outputs of other neurons in a larger system). Diverging inputs and/or steering the coupled modular system into unstable synchronization domains are different techniques for de-synchronization.

References

[1] Kapitaniak, T. (1996). *Controlling Chaos - Theoretical and Practical Methods in Non-linear Dynamics.* San Diego: Academic Press.

[2] Pasemann, F. (1995). Neuromodules: A dynamical systems approach to brain modelling. In H. Herrmann, E. Pöppel, D. Wolf (eds.), *Supercomputing in Brain Research - From Tomography to Neural Networks*, (pp. 331–347). Singapore: World Scientific.

[3] Rössler, O. (1979) An equation for hyperchaos. *Phys. Lett. A*, **71**, 155-157.

[4] Singer, W. (1994) Time as coding space in neocortical processing. In Buzsáki, G.; Llinás, R.; Singer, W.; Berthoz, A. and Christen, Y. (eds.) *Temporal Coding in the Brain.* Springer, Berlin. pp. 51-80.